The 5th International Symposium on Applied Electromagnetics – SAEM'2014

Skopje, Macedonia, June 8-11, 2014

Efficiency Optimisation of Single Phase Motor Using GA Approach

Vasilija Sarac[1], Goga Cvetkovski[2]

[1] Goce Delcev Univsersity Electrotechnical Faculty, P.O.Box 201, 2000 Stip, Macedonia, vasilija.sarac@ugd.edu.mk

[2] Ss. Cyril and Methodius University, Faculty of Electrical Engineering and Information Technologies, P.O. Box 574, 1000 Skopje Macedonia, gogacvet@feit.ukim.edu.mk

Abstract ***In this paper Genetic Algorithm for efficiency optimisation of single phase shaded pole motor is implemented. For this purpose an extensive mathematical model of the motor is developed. The efficiency of the motor as an objective function of the optimisation is selected. The optimisation process is performed for different set of optimisation parameters (three, four and five variables). The prototype as well as the optimised motor models afterwards are modelled and analysed using Finite Element Method. An analysis of the magnetic field distribution, as well as flux density values, in the whole cross-sectional area of all models has been performed in order to validate the improvements of the optimised models in relation to the basic motor model.***

1 Introduction

Induction motors are widely used in industry since they are rugged inexpensive and maintenance free. It is estimated that more than 50 % of the world generated electric energy is consumed by electrical machines. Improving efficiency in electrical motors is important from economical point of view, as well as from the point of reduction of environmental pollution [1]. Single phase shaded pole motor belongs to the most widespread single phase motor, due to robust and reliable construction and low production costs, although its operational characteristics are not its strong side. Here are some common values for this type of motor: efficiency η (0.25÷0.4) and power factor $cos\varphi$ (0.4÷0.6). Very important feature about this type of single phase motor is that the locked rotor current has a very close value to rated current meaning that motor is capable of sustaining overload or full load at locked rotor position which makes it irreplaceable driving force, especially in applications where a large starting torque is not required. In this paper the authors propose a methodology for improving the efficiency of this type of motor using Genetic Algorithm (GA) as an optimisation tool in the optimal design of AKO-16 motor (Fig.1) product of MicronTech Company. Firstly, an analytical model of the motor is developed based on the revolving field theory and current symmetrical components. The analytical model accuracy is verified using experimental and manufacturer test data. After the GA optimisation the basic motor model (BM) is improved with three motor models using different number of optimisation parameters. The first motor model is optimised with three variables (M1), the second (M2) and third motor (M3) model are optimised with four and five variables, respectively. The aim of the GA optimisation is to maximise the efficiency of the motor, which is the objective function of the optimisation. The evaluation of all motor models is done using the Finite Element Method (FEM) analysis.

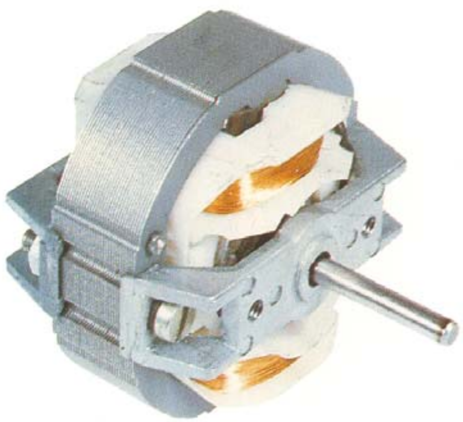

Fig.1. Motor physical layout

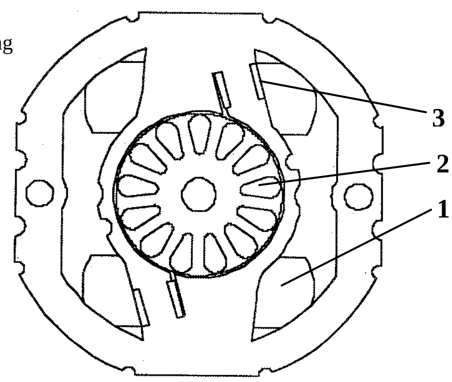

Fig.2. Motor cross-section

2 GA method results

Genetic Algorithm has proved itself during recent years as a reliable, robust optimisation technique that enables to obtain a global optimum of certain function by performing optimisation search over many families of possible solutions thus avoiding location of one optimal solution which may not necessarily be the global optimum. Defining the input variables of the analytical motor model is the first step in the GA programming. The efficiency of the motor is chosen to be the objective function for optimisation. Optimisation is performed without changing motor outer dimensions which is important from mounting point of view. First motor model which is considered to be basic motor model (BM) is derived from motor mathematical model for the prototype. All optimized motor models have different number of variables. The first motor model–M1 has three optimisation parameters, the second model-M2 has four and the third motor model-M3 has five variable optimisation parameters. In Table 1 the ranges of variation of the input variables for all motor models, as well their values after the optimisation are presented. Optimisation is performed for rated operating point for motor slip *s*=0.16.

Table 1. Ranges of variation of GA parameters

	BM	Variation range	M1 output	M2 output	M3 output
Current density Δ (A/mm^2)	8	5 ÷ 10	5.17	5.045	5
Air gap flux density B_δ(T)	0,404	0.4 ÷ 0.45	0.40035	0.40035	0.4
Angle of rotor skew α_{sk} (°)	17	15 ÷ 20	15.025	15.008	15.0035
Width of stator pole b_p (m)	0,016	b_p=0.012 ÷ 0.02	0.016=const	0.016=const	0.012
Shading portion of stator pole a (/)	0,25	*a*=0.2 ÷ 0.4	0.25=const	0.2	0.2

The obtained parameters from the GA optimisation afterwards are used for calculation of motor parameters and characteristics for all motor models. They are presented in Table 2 and Table 3. In Table 3 are presented motor parameters such as: current density-Δ, air gap flux density B_δ, angle f skew of rotor bars α_{sk}, diameter of copper wire in main stator winding-d_{cu}, number of turns in main stator winding-*W*, active and reactive resistance in main stator winding R_1 and X_1, in short circuit coil R_3 and X_3, in rotor winding R_2 and X_2, mutual reactance between stator windings X_{12} and between main stator winding and rotor X_{13}. All important motor operational characteristics are calculated for different slip *s* for the whole motor operating range (0÷1) for all motor models. Comparative characteristics of electromagnetic torque, input power and output power are presented in Figure 3, Figure 4 and Figure 5, respectively.

Table 2. Motor models characteristics

Quantity	BM	M1	M2	M3	Experim.	Producer
Stator current I_1 (A)	0.126	0.131	0.128	0.1235	0.129	0.11±10%
Rotor current I_2 (A)	0.0875	0.092	0.0941	0.09316	/	/
Short circuit coil I_3(A)	0.00643	0.00667	0.0046	0.0048	/	/
Power factor cosφ (/)	0.654	0.59224	0.6283	0.643	0.667	0.6376
Input power P_1 (W)	18.11	17.14	17.74	17.46	19.1	16±10%
Output power P_2 (W)	4.149	4.73	5.61	6	/	/
Torque M_{em} (mNm)	18.075	20.28	23.6	25.1	/	/
Efficiency factor η (/)	0.229	0.276	0.31	0.35	/	/

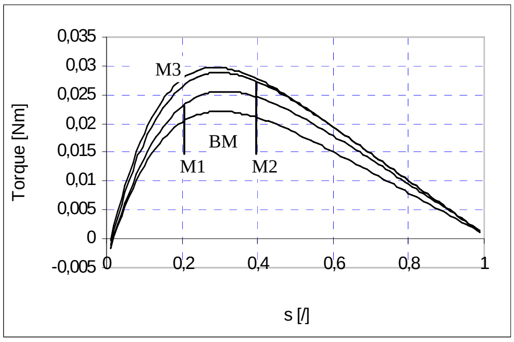

Fig. 3 Electromagnetic torque characteristics

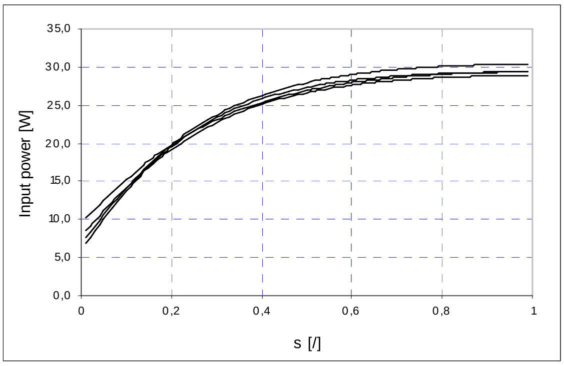

Fig.4. Input power characteristics

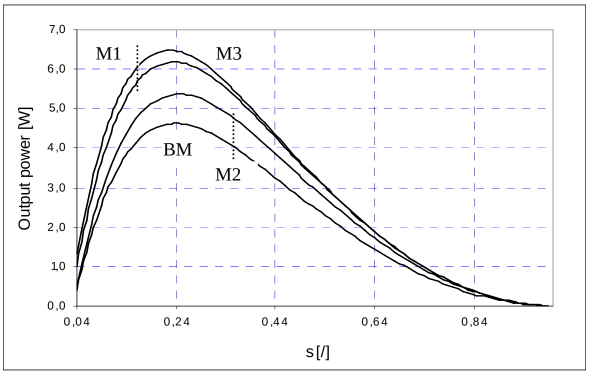

Fig.5. Output power characteristics

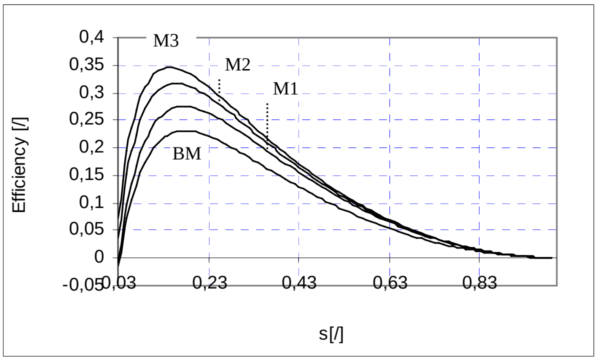

Fig.6. Efficiency characteristics

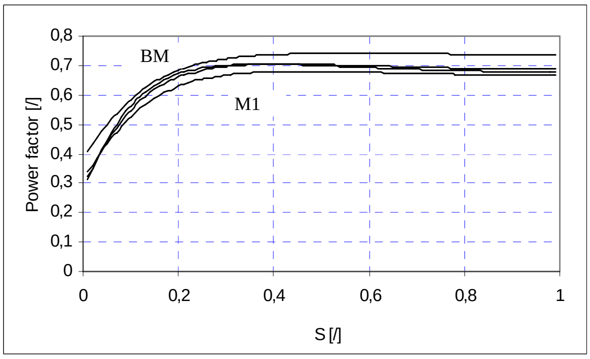

Fig.7. Power factor characteristics

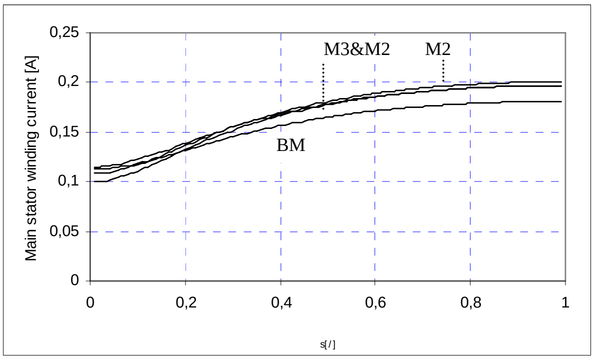

Fig.8. Characteristics of main stator winding current

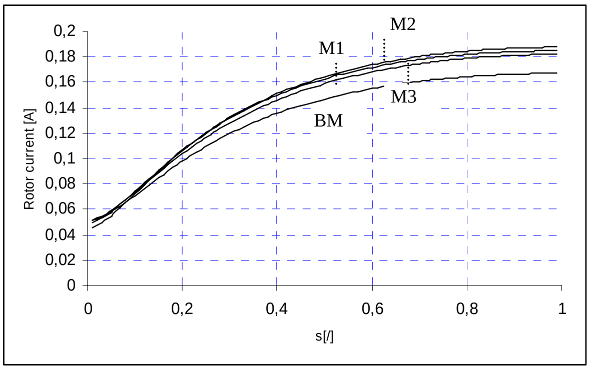

Fig.9. Characteristics of rotor winding current

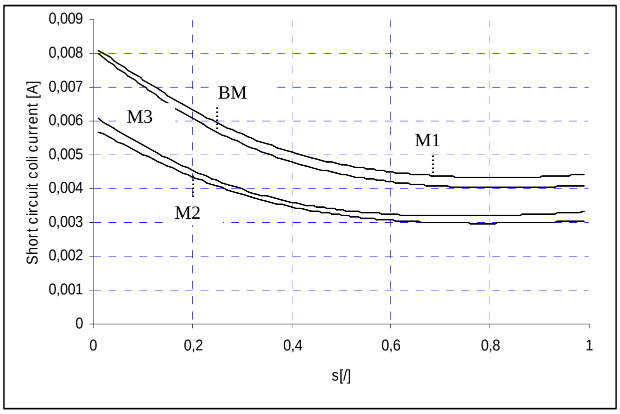

Fig.10.Characteristics of short circuit coil current

Table 3. Motor models parameters

BM	M1	M2	M3
Δ=5 (A/m^2)	Δ=5.17 (A/m^2)	Δ=5.0 (A/m^2)	Δ=5 (A/m^2)
B_δ=0.404(T)	B_δ=0.40035(T)	B_δ=0.4003(T)	B_δ=0.4 (T)
α_{sk}=17 (^{0})	α_{sk}=15.0025(^{0})	α_{sk}=15.008(^{0})	α_{sk}=15.003 (^{0})
d=2,4(mm)	d=1,8(mm)	d=1.8(mm)	d=1.8(mm)
bp=0,016(m)	bp=0,016(m)	bp=0,016(m)	bp=0,012 (m)
a=0.25	a=0.25	a=0.2	a=0.2
d_{cu}=0.14(mm)	d_{cu}=0.18 (mm)	d_{cu}=0.18(mm)	d_{cu}=0.18 (mm)
W=3488 turns	W=3520 turns	W=3520 turns	W=3522 turns
R_1=492.98 Ω	R_1=330.5 Ω	R_1=341.89 Ω	R_1=341.95 Ω
X_1=498.17 Ω	X_1=515.83 Ω	X_1=462.68 Ω	X_1=449.13 Ω
R_2=497.04 Ω	R_2=458 Ω	R_2=457.93 Ω	R_2=458.54 Ω
X_2=76.71 Ω	X_2=78.12 Ω	X_2=89.3 Ω	X$_2$=99.47 Ω
R_3=18474 Ω	R_3=18814.8 Ω	R$_3$=28234.4 Ω	R_3=27292.3 Ω
X_3=127.53 Ω	X_3=129.87 Ω	X_3=127.46 Ω	X_3=125.18 Ω
X_{12}=2163.3 Ω	X_{12}=2202.97 Ω	X_{12}=2518.4 Ω	X_{12}=2804.87Ω
X_{13}=175.91 Ω	X_{13}=179.13 Ω	X_{13}=183.84 Ω	X_{13}=220.12 Ω

In Figure 6, Figure 7, and Figure 8 comparative characteristics of efficiency factor, power factor and main stator winding current for all motor models are presented, while in Figure 9 and Figure 10 comparative characteristics of rotor winding current and short circuit coil current are presented, respectively. Compared to authors previous work [2], in this case when the efficiency is adopted as objective function of the optimisation the increase of the efficiency is achieved by increasing the motor output power without increasing the motor power consumption, for the same value of the power factor for rated operational point which is important for the energy savings. The small modifications in motor inner construction contributed in the increase of the motor output power, as well as improved motor efficiency. The increase of efficiency is followed by increase of electromagnetic torque which is also important from operational point of view. In Table 4 percentage increase of efficiency and electromagnetic torque in optimised motor models compared to the basic motor model is presented.

Table 4. Comparison of efficiency factor at different motor models

	BM	M1	M 2	M3
Electromagnetic torque M_{em} (Nm)	0.018	0.0202	0.0236	0.0251
Improvement of electromagnetic torque compared to the basic motor model (%)	-	12	31	39.4
Efficiency (/)	0.229	0.276	0.31	0.35
Improvement of efficiency factor compared to the basic motor model (%)	-	20.5	35.3	52.8

3 FE method results

Motor model is input in FE program for calculation of magnetic flux density in motor cross-section as well as motor air gap for different operating regimes. Motor exact geometry is input, boundary condition are defined which in this case a Dirchlet boundary conditions. The most common use of Dirichlet-type boundary conditions in magnetic problems is to define $A = 0$ along a boundary to keep magnetic flux from crossing the boundary. Materials in all motor regimes are defined including the non-linearity of magnetic material and magnetic core laminations [3]. Time harmonic analysis is run at frequency f=50 Hz. Current density in main stator winding is input while in short circuit coil and rotor cage currents are freely induced. Rotor bars conductivity is adjusted according to motor slip. In Figure 11, Figure 12, Figure 13 and Figure 14 magnetic flux density distribution in all motor models at no-load is presented.

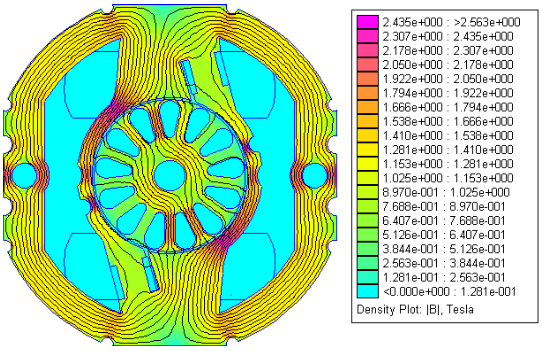

Fig.11.Magnetic flux distribution for BM-no load

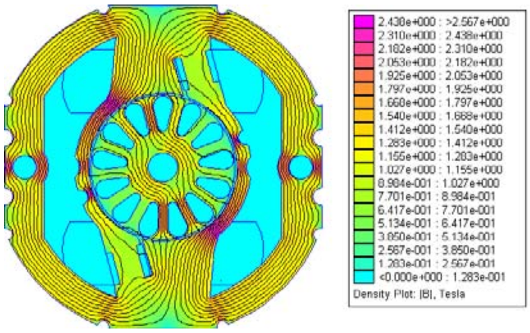

Fig.12.Magnetic flux distribution for M1-no load

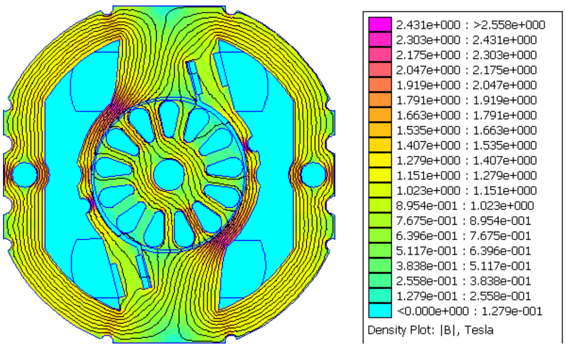

Fig.13.Magnetic flux distribution for M2-no load

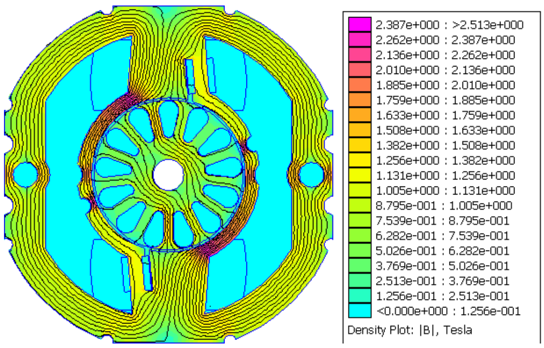

Fig.14.Magnetic flux distribution for M3-no load

Magnetic flux density distribution in all motor models has shown a slight decrease in the values in the optimised motor models proving that stator bridge is a "week" point in motor construction experiencing in some points high values of magnetic flux density. In model M3 values of magnetic flux density are decreased in almost all motor cross-section area except of stator bridge compared to other motor models and distribution of magnetic flux density is more equally distributive with no points of high saturation outside the stator bridge. Distribution of magnetic flux density in motor air gap for no-load operating regime is calculated and it is presented in Figure 15, Figure 16, Figure 17 and Figure 18.

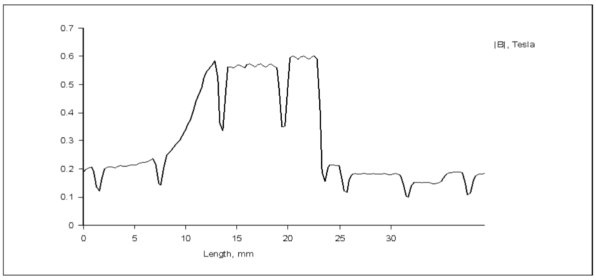

Fig.15. Air gap flux density distribution for BM-no load

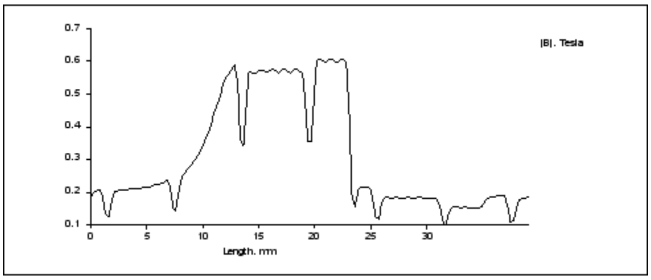

Fig.16. Air gap flux density distribution for M1-no load

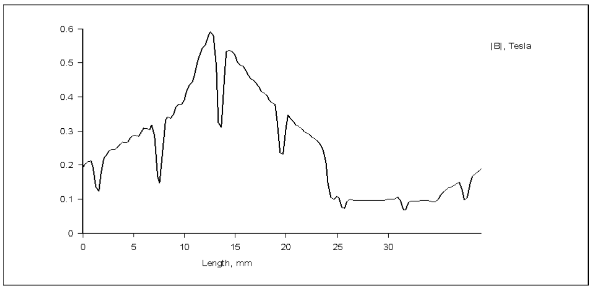

Fig.17. Air gap flux density distribution for M2-no load

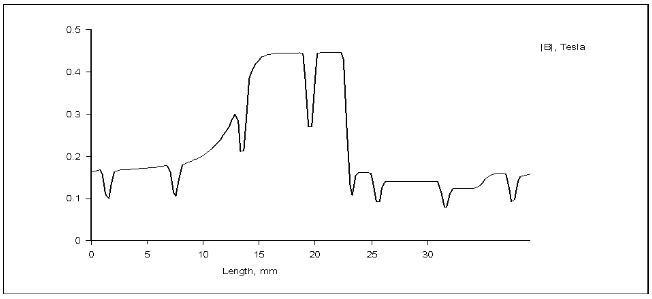

Fig.18. Air gap flux density distribution for M3-no load

In Table 4 are presented maximal and minimal values of magnetic vector potential A_{max} and A_{min} as well as maximal value of magnetic flux density in motor core cross-section B_{max}, flux per pole – Φ as well as flux linkage – F for no-load operating conditions.

Table 5. Flux density and magnetic vector potential at no-load

Parameter	BM	M1	M2	M3
A_{max} (Vs/m)	7.2x10^{-3}	7.3x10^{-3}	6.3x10^{-3}	5.6x10^{-3}
A_{min} (Vs/m)	-7.2x10^{-3}	-7.3x10^{-3}	-6.3x10^{-3}	-5.2x10^{-3}
B_{max} (T)	2.435	2.438	2.431	2.387
Flux per pole (Vs)	1.32x10^{-4}	1.34x10^{-4}	1.24x10^{-4}	1.24x10^{-4}
Flux linkage (Vs)	0.461	0.471	0.437	0.436

All motor models are also analysed for rated load operating conditions. For that purpose appropriate current densities are inputted in main stator winding and rotor bars conductivity is modelled according to motor slip. Results of magnetic flux distribution at rated load for models BM and M1 are presented in Figure 19 and Figure 20 and for motor models M2 and M3 in Figure 21 and Figure 22, respectively.

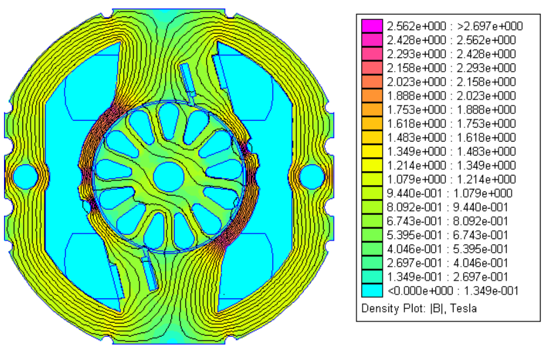

Fig.19. Magnetic flux distribution for BM-rated load

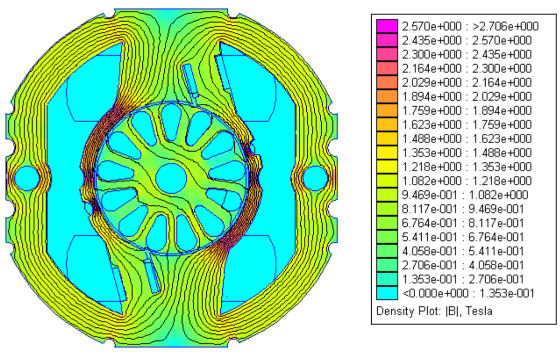

Fig.20. Magnetic flux distribution for M1-rated load

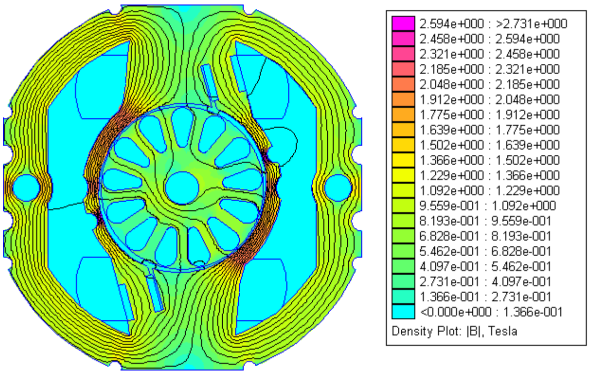

Fig.21. Magnetic flux distribution for M2-rated load

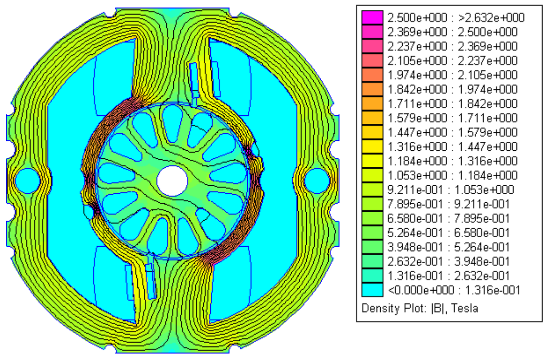

Fig.22. Magnetic flux distribution for M3-rated load

Calculation of magnetic flux density at rated load conditions has shown decreased values of magnetic flux density in optimized model M3 with areas of high values of magnetic flux density in stator bridge. Distribution of magnetic flux density in motor air gap for all motor models at rated load is presented in Figure 23, Figure 24, Figure 25 and Figure 26.

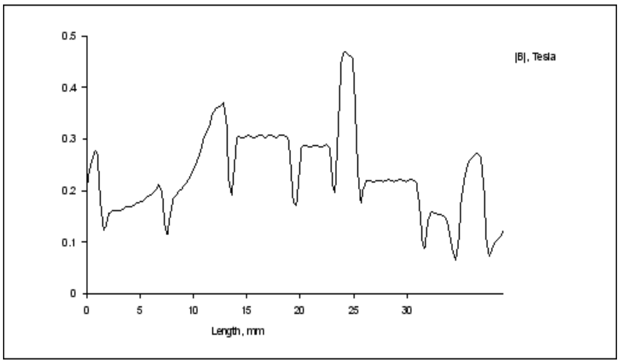

Fig. 23. Air gap flux density distribution for BM-rated load

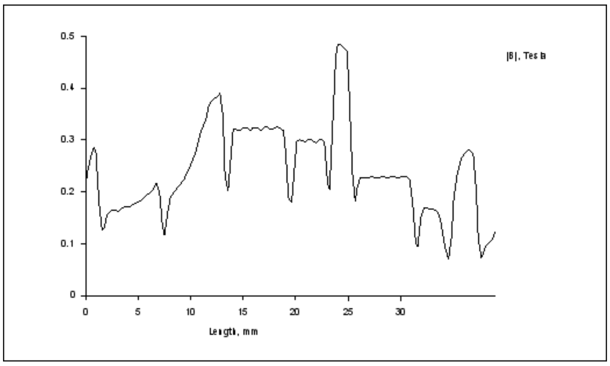

Fig. 24. Air gap flux density distribution for M1-rated load

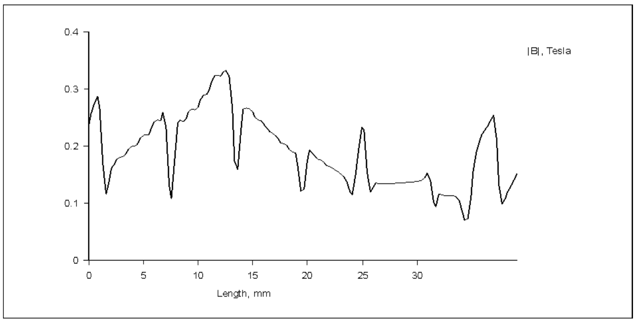

Fig. 25. Air gap flux density distribution for M2-rated load

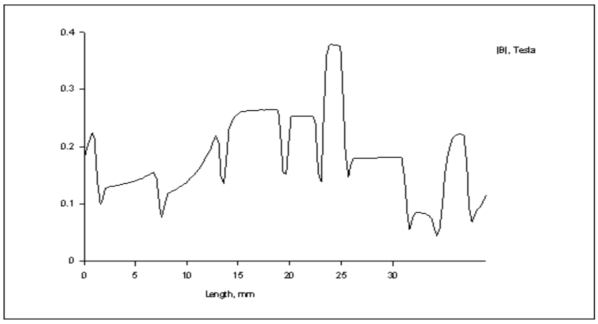

Fig. 26. Air gap flux density distribution for M3-rated load

In Table 6 maximal and minimal values of magnetic vector potential A_{max} and A_{min} as well as maximal value of magnetic flux density in motor core cross-section B_{max}, flux per pole – Φ as well as flux linkage – F, for rated load operating conditions are presented.

Table 6. Flux density and magnetic vector potential at rated load

Parameter	BM	M1	M2	M3
A_{max} (Vs/m)	5.1x10^{-3}	5.3x10^{-3}	5.4x10^{-3}	4.4x10^{-3}
A_{min} (Vs/m)	-5.1x10^{-3}	-5.3x10^{-3}	-3.7x10^{-3}	-4.4x10^{-3}
B_{max} (T)	2.594	2.57	2.594	2.5
Flux per pole (Vs)	0.98x10^{-4}	1.04x10^{-4}	0.88x10^{-4}	0.7x10^{-4}
Flux linkage (Vs)	0.343	0.366	0.309	0.25

Soft magnetic material is implemented only in construction of stator bridge, in order to be improve magnetic flux density distribution in motor cross-section. Obtained results for motor models BM and M3 at rated load operating condition are presented in Figure 27 and Figure 28. From the presented results it can be concluded that magnetic flux density in stator bridge for both motor models is considerably lowered and with this action the high saturation of magnetic material in this critical part of motor is avoided.

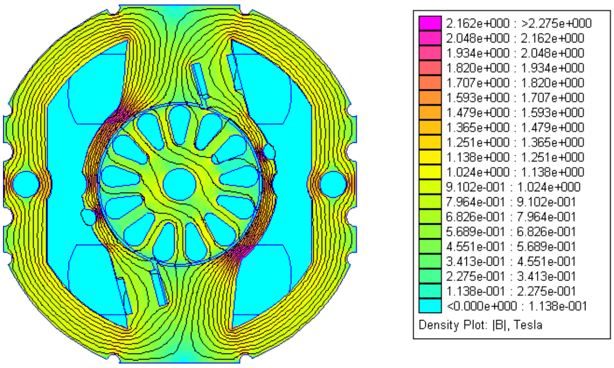

Fig.27. Magnetic flux distribution for BM at rated load and application of soft magnetic material in stator bridge

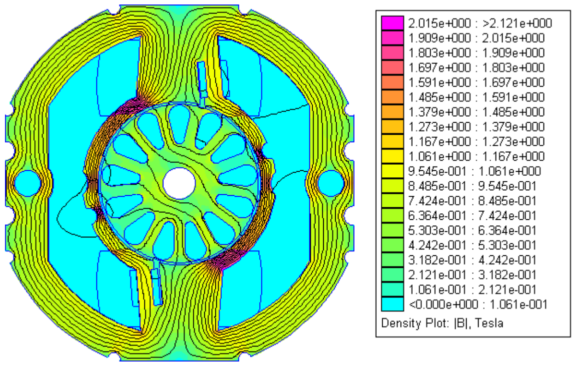

Fig.28. Magnetic flux distribution for M3 at rated load and application of soft magnetic material in stator bridge

4 Conclusion

Single phase shaded pole motor belongs to a group of small motors well-know for its robust construction and reliability, but also known as motor with relatively poor efficiency and power factor. For that reason an optimisation procedure was performed using genetic algorithms as a tool. The efficiency of the motor was defined as an objective function for the optimisation. By improving the value of the motor efficiency the value of the power factor and electromagnetic torque without changing the motor outer dimensions was also improved. The optimisation model is developed based on method of symmetrical components with gradual increase of number of varied parameters from three up to five. The results form the optimisation procedure have proved gradual increase of the efficiency of the motor of 20.5% in the first optimised model, 35.3% in the second model and up to 52.8% in the last optimised model which utilizes five input variable parameters. The increase of the efficiency is followed by increase of electromagnetic torque of 12% in the first model, 31% in the second and 39.4% in the third optimised motor model. The increase of the efficiency is obtained without increasing the motor input power, that is 18 W in all motor models, which is important from the aspect of power consummation, but at the same time output power is considerably increased from 4.2 W in the basic model up to 6 W in the third optimised motor model. The value of the power factor is maintained almost at the same level in all motor models. Magnetic flux density in the motor cross-section, as well as in motor air gap, is calculated and presented using Finite Element Method. Two different operating regimes were investigated: rated load and no-load. In both regimes by using the FE method it was concluded that the stator bridge is experiencing high values of magnetic flux density and magnetic material saturation in the basic, as well as in optimised motor models. Therefore, soft magnetic material is placed in the construction of the stator bridge which considerably lowered the magnetic flux density in this saturated part of the motor construction regarding high values of flux densities.

References

[1] W. Leonhard, “Controlled AC Drives, a Successful Transfer from Ideas to Industrial Practice,” *Control Engineering Practice*, Vol. 4, No. 7, 1996, pp. 897-908.

[2] V. Sarac, G. Cvetkovski, ”Different Motor Models Based on Parameter Variation Using Method of Genetic Algorithms”, *Journal Przeglad Electrotechniczn* , 87, NR 3/2011, pp. 162-166.

[3] David Meeker “Finite Element Method Magnetics”, Version 4.2, User’s Manual.